ACCURACY OF RADIONUCLIDE CEREBRAL ANGIOGRAMS IN THE DETECTION OF CEREBRAL ARTERIOVENOUS MALFORMATIONS

J. Wendell Tyson*, Lynn R. Witherspoon†, R. H. Wilkinson, Jr., and Jack K. Goodrich

Duke University Medical Center and Veterans Administration Hospital, Durham, North Carolina

Radionuclide cerebral angiography is demonstrated to be a sensitive screening procedure for the presence of intracerebral arteriovenous malformations. The characteristic findings are increased radionuclide activity at the site of the lesion in the arterial phase followed by a rapid decline in radionuclide activity following the venous phase. This pattern may also be observed in malignant gliomas and following cerebral infarction. The radionuclide cerebral angiogram should not be used as the sole method of establishing the diagnosis of an arteriovenous malformation.

Arteriovenous malformations (AVMs) of the brain are responsible for 8% of patients presenting with subarachnoid hemorrhage and represent 1.5–4% of verified intracranial tumors (*1*). Patients with AVMs frequently present with such nonspecific symptoms as headaches or seizures (*2*). The desirability of reaching an accurate diagnosis in such patients without subjecting all to more hazardous diagnostic procedures prompted the investigation of radionuclide cerebral angiography as a screening procedure (*3*). Recent reports have suggested that a characteristic pattern of cerebral tracer distribution is seen in AVMs that is not commonly observed in vascular neoplasms (*3–6*). Although both lesions may show early arterial phase activity, vascular neoplasms are reported to exhibit slower "washout" of activity during the venous phase of the radionuclide angiogram and subsequently to retain more of the tracer material. This study was undertaken to evaluate the diagnostic accuracy of radionuclide cerebral angiograms in patients with proven AVMs. The radionuclide cerebral angiographic findings in patients with AVMs were defined. Other conditions in which similar cerebral radionuclide angiogram findings were observed including a vascular neoplasm demonstrating considerable shunting are discussed.

MATERIALS AND METHODS

Forty-three patients with histologic or angiographically proven AVMs of the brain were studied with static brain scans and contrast carotid arteriograms. Of these, 16 patients had radionuclide cerebral angiograms preceding their static brain scans. Eight males and eight females ranging in age from 14 to 76 years were studied. Radionuclide cerebral angiograms were performed following the intravenous bolus injection of 20–30 mCi of ^{99m}Tc-pertechnetate. We are presently performing the injections using the technique of Lane, et al (*7*). Fifteen patients were studied using a single-crystal scintillation gamma camera equipped with a data storage system (Searle Radiographics Pho/Gamma HP with videotape recorder or Nuclear Data Radicamera with Med II). Scintiphotographic images were obtained at 1.2–3 sec intervals of each study. Area-of-interest cerebral hemispheric activity versus time curves was constructed in selected patients. The areas of interest were selected to include the AVM in the abnormal hemisphere and an equal area in the contralateral hemisphere. Area-of-interest curves generated from videotape were recorded by a dual ratemeter stripchart recorder at a speed of 8 in./min using a 0.5-sec time constant. One patient (Case 12, Table 1) was studied using a multicrystal imaging device (Baird-Atomic System 70) and similar area-of-interest curves were obtained using the system's data-processing computer. Patients were routinely positioned in the anterior projection unless clinical signs or history indicated a posterior lesion. Static

Received April 30, 1974; original accepted June 4, 1974.

For reprints contact: Jack K. Goodrich, Division of Nuclear Medicine, Duke University Medical Center, Durham, North Carolina 27710.

* Present address: Division of Nuclear Medicine, Louisville General Hospital, Louisville, Ky. 40202.

† Present address: Department of Nuclear Medicine, Ochsner Foundation Hospital, New Orleans, La. 70121.

brain images were obtained 30–60 min following injection using a dual-probe 5-in. rectilinear scanner (Ohio-Nuclear Model 54 or Raytheon dual-probe scanner).

Radionuclide cerebral angiograms were divided into four phases for the purposes of characterizing these lesions. The arterial phase is characterized by the presence of radionuclide activity in the carotid, anterior, and middle cerebral arteries. A brief capillary phase is characterized by diffuse hemispheric activity seen between the disappearance of the arterial phase and the appearance of the venous phase. The venous phase is characterized by the appearance of radionuclide activity in the superior sagittal sinus, the transverse sinuses, and the jugular veins. An equilibrium phase is observed after the disappearance of the venous phase.

Contrast carotid arteriograms were usually performed within 48 hr after the radionuclide cerebral angiogram was obtained.

Three case reports are presented, two of which illustrate the radionuclide cerebral angiogram findings seen in arteriovenous malformation. The three cases include an atypical frontal lobe AVM, which arteriographically simulated a malignant glioma, an occipital lobe AVM with classical findings, and a malignant glioma, which demonstrated the same cerebral radionuclide distribution pattern seen in AVMs in this series.

RESULTS

Findings on the radionuclide cerebral angiograms, brain scans, and contrast carotid arteriograms in 16 patients with AVMs were reviewed and the results are summarized in Table 1.

CASE REPORTS

The first patient (Case 4, Table 1) is a 23-year-old woman who presented with intermittent headaches of 5 years' duration. The general physical examination was within normal limits. Neurologic examination revealed no focal signs. Skull radiographs were within normal limits. The radionuclide

TABLE 1. FINDINGS IN 16 CASES OF INTRACRANIAL ARTERIOVENOUS MALFORMATION

Case No.	Age (yr)	Sex	Presenting symptoms	Scan	RCA results	Carotid arteriogram
1	14	M	Focal seizures	Pos. lt. parietal	Pos. lt.	Lt. parietal AVM fed by post-parasagittal branch MCA
2	19	M	Headaches and visual disturbance	Pos. lt. parietal	Pos. lt.	Lt. parietal AVM fed by MCA
3	23	F	Seizures since childhood	Pos. rt. frontal	Pos. rt.	Rt. frontal AVM fed by fronto-parietal branch of MCA
4	23	F	Headaches	Negative	Pos. rt.	Rt. frontal glioma (surgical and histologic diagnosis of AVM)
5	24	F	Headaches, seizures, and subarachnoid hemorrhage	Pos. lt. parietal	Pos. lt.	AVM lt. parietal lobe fed by ACA, MCA, and PCA
6	25	M	Seizures	Pos. rt. frontal	Pos. rt.	AVM rt. frontal lobe fed by ACA and MCA
7	39	F	4-mo. history of seizures	Pos. lt. occipital	Pos. lt.	Lt. post-temporal AVM fed by PCA
8	41	M	4-yr history of headaches	Pos. rt. parietal	Pos. rt.	Rt. parietal AVM fed by MCA and ACA
9	44	M	Seizure disorder	Pos. lt. temporal	Pos. lt.	Lt. temporal fossa AVM fed by lt. MCA
10	49	F	1-yr history of lt. facial headaches	Pos. lt. occipital	Pos. lt.	Lt. occipital AVM fed by lt. MCA
11	55	M	4-wk history lt. frontal headaches	Pos. lt. frontal	Pos. lt.	Lt. frontal AVM and aneurysm AVM fed by lt. MCA
12	58	M	Headaches, subarachnoid hemorrhage	Pos. rt. frontal	Pos. rt.	Rt. frontal AVM fed by rt. MCA and ACA
13	60	F	Roaring in ears	Pos. lt. temporal	Pos. lt.	Lt. temporal AVM fed by lt. MCA
14	62	M	Headaches, amnesia	Pos. lt. subfrontal	Pos. lt.	Lt. subfrontal AVM fed by lt. MCA and ACA
15	73	F	3-yr history of seizures	Pos. lt. parietal	Pos. lt.	Lt. parietal AVM fed by lt. MCA
16	76	F	2-yr history of roaring in ears	Pos. rt. occipito-parietal	Pos. rt.	Rt. dural AVM fed by rt. vertebral, PCA and ICA

Legend: RCA, Radionuclide cerebral angiogram; AVM, Arteriovenous malformation; MCA, Middle cerebral artery; PCA, Posterior cerebral artery; ACA, Anterior cerebral artery; ICA, Internal carotid artery.

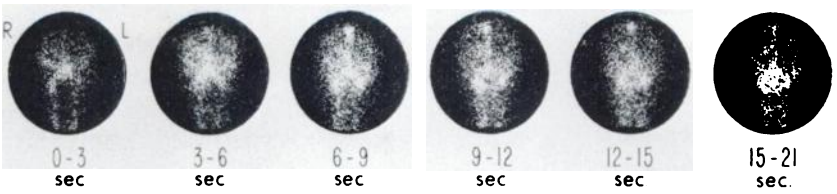

FIG. 1. Frontal lobe AVM demonstrates arteriographic appearance of glioma. Anterior view.

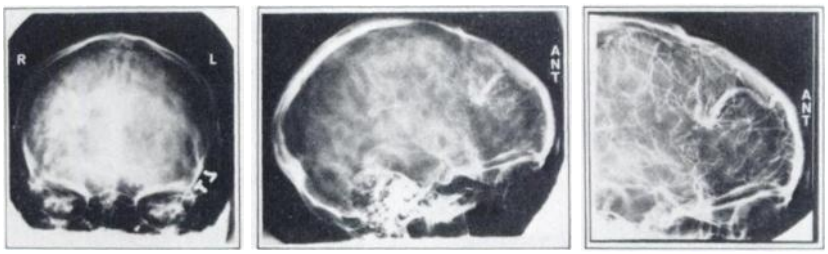

FIG. 2. Arteriogram of AVM shown in Fig. 1 shows malformation.

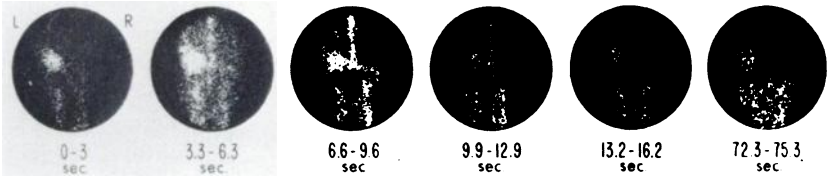

FIG. 3. Occipital lobe AVM. Posterior view.

cerebral angiogram revealed an area of abnormally increased radionuclide activity in the right hemisphere early in the arterial phase with decreasing activity in this area following the venous phase (Fig. 1). The brain scan was within normal limits. Later the same day a right serial carotid arteriogram was obtained and was interpreted as showing a deep right frontal glioma. Arteriographically the lesion demonstrated numerous medullary veins, apparent neovascularity, slight mass effect, large draining veins, and no appreciable arteriovenous shunting (Fig. 2). Interpretation was based on the criteria of Goree and Dukes (*8*). Three days later a right frontal osteoplastic craniotomy was performed. During the course of surgery it became evident that the lesion was an arteriovenous malformation rather than a malignant neoplasm. The arteriovenous malformation extended to the roof of the right lateral ventricle and was fed by a branch from the right anterior cerebral artery. Microscopic examination revealed involvement of both the gray and white matter of the cerebral cortex. The white matter underlying the lesion contained increased numbers of thin-walled vessels separated by unremarkable brain tissue. The final histologic diagnosis was arteriovenous malformation composed almost entirely of venous elements. The patient was subsequently discharged in satisfactory condition. She was last seen 10 months following surgery at which time she was on seizure medication and experiencing no seizure activity. No additional neurologic abnormalities were detected at the time of her followup examination.

The second patient (Case 10, Table 1) is a 49-year-old woman who presented with a 1-year history of left facial headaches, a left carotid bruit, and bilateral ocular bruits. A posterior radionuclide cerebral angiogram revealed marked increased radionuclide activity in the left occipital area during the arterial phase and rapid decline of this activity following the venous phase (Fig. 3). The brain scan also revealed a 3-cm area of abnormally increased radionuclide activity corresponding to the abnormal activity seen on the radionuclide cerebral angiogram. A left brachial arteriogram demonstrated an AVM of the left occipital lobe fed by the left middle cerebral artery (Fig. 4). The area-of-interest activity versus time curves constructed from the radionuclide cerebral angiogram illustrates marked increase in activity in the region of the AVM compared with the opposite hemisphere (Fig. 5).

The third patient is a 54-year-old man who presented with visual disturbance, headaches, papilledema, right-sided weakness, and progressive dementia. A posterior radionuclide cerebral angiogram demonstrated abnormal radionuclide activity in the left posterior parietal area in the arterial phase, which disappeared rapidly following the venous phase (Fig. 6). The brain scan demonstrated an irregular area of abnormally increased radionuclide activity in the same area. The area-of-interest activity versus time curves constructed from the radio-

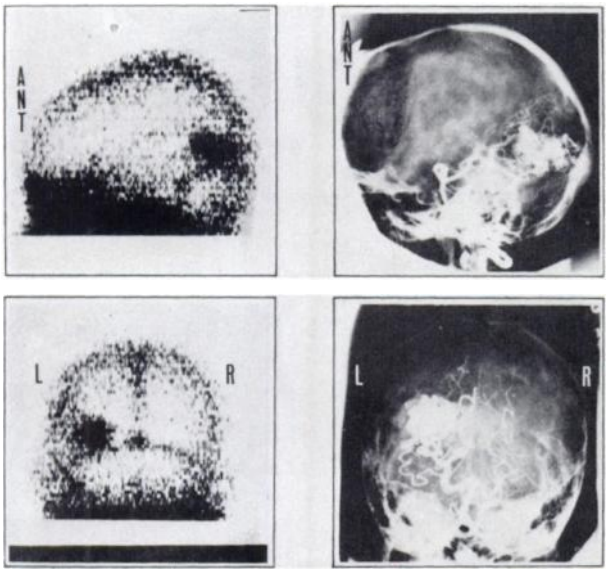

FIG. 4. Brain scan and arteriogram of occipital lobe AVM. (Top row) Left lateral; (bottom row) posterior view.

nuclide cerebral angiogram illustrates marked increase in activity in the region of the tumor compared with the opposite hemisphere (Fig. 7). A serial left carotid arteriogram demonstrated a vascular glioma in the left posterior parietal region with shunting to numerous superficial cortical veins and to the vein of Labbé inferiorly (Fig. 8). This area of brain was removed surgically, and histologically, it was a glioblastoma multiforme.

DISCUSSION

All 16 arteriovenous malformations in this series were demonstrated by radionuclide cerebral angiography. None of the patients studied had a lesion less than 2 cm in diameter. The overall reported incidence of radionuclide cerebral angiographic demonstration of arteriovenous malformations including our series is 96% (Table 2). There are two reported cases of a normal radionuclide cerebral angiogram in patients with proven arteriovenous malformations. In both instances these lesions were small. Landman and Ross (*3*) reported that in their case the lesion was less than 1 cm in diameter and surrounded by a hematoma. Meschan, et al (*9*) did not state the exact size of their lesion.

The characteristic radionuclide cerebral angiographic pattern seen in our series of AVMs was a rapid accumulation of radionuclide activity at the site in the arterial phase followed by rapid decline of radionuclide activity in this area immediately following the venous phase (Fig. 3). This may be further characterized by region-of-interest activity versus time curves as illustrated in Fig. 5. It has been suggested that this pattern is typical of arteriovenous malformations (*3–6*). Although this radionuclide accumulation pattern was seen in all AVMs in this series, it is not specific for this lesion.

Increased arterial phase activity is observed in some malignant intracranial neoplasms. In our series of 150 radionuclide cerebral angiograms performed in 32 patients with anaplastic intracerebral gliomas, we have observed increased arterial phase activity at the site of the lesion in 29 studies. In 28 of these 29 studies moderate increased arterial phase activity was followed by slight venous phase decline and then marked tracer accumulation during the equilibrium phase. In only one study was marked increase in radionuclide activity in the arterial phase followed by decline in activity after the venous phase characteristic of arteriovenous malformation observed (Fig. 7). In this glioma there was extensive shunting to cortical veins as well as to the vein of Labbé. This unusual amount of shunting may explain the decline in activity observed following the venous phase. Extensive equilibrium phase tracer accumulation resulted in a markedly positive brain scan. This latter finding suggested the true nature of the lesion.

Yarnell, et al (*12*) have reported increased arterial phase radionuclide activity observed by radionuclide cerebral angiography in 13 patients following cerebral infarction. Their illustrations of these "hot strokes" appear similar to the findings reported in AVMs. Angiographically this finding probably corresponds to increased neovascularity and arteriovenous shunting as described by Lassen (*13*). This finding in cerebrovascular occlusive disease may be relatively uncommon but must be considered in the

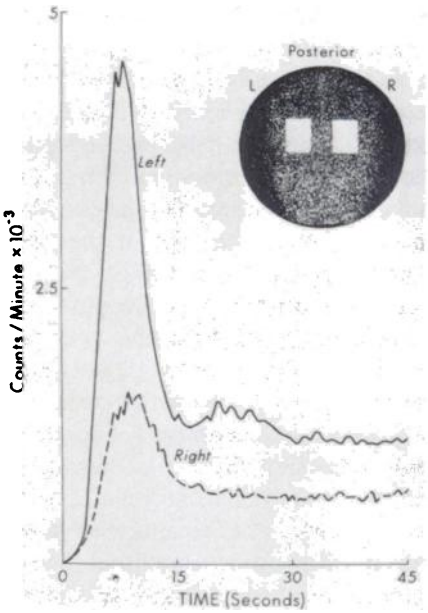

FIG. 5. Activity versus time curves of AVM shown in Figs. 3 and 4.

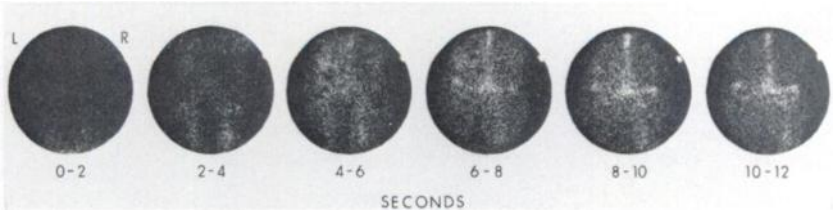

FIG. 6. Left occipitoparietal lobe glioblastoma multiforme shows appearance of AVM by radionuclide cerebral angiogram. Posterior view.

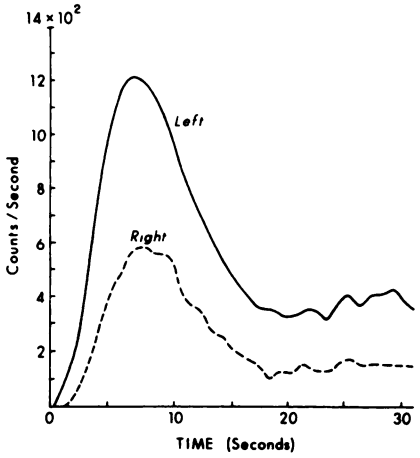

FIG. 7. Activity versus time curves of left occipitoparietal glioblastoma multiforme.

differential diagnosis of increased arterial phase activity seen on radionuclide cerebral angiography.

It has been reported that the shape of the lesion as demonstrated by brain scan together with the typical AVM radionuclide cerebral angiogram pattern may be of some value in predicting the nature of the lesion (*3*). Radionuclide accumulation seen on brain scans in patients who have AVMs is reported to be more irregular than that seen in tumors. In individual cases we have not found this to be helpful. In our experience and that of Cowan (*6*) no lesion with a radionuclide cerebral angiogram demonstrating increased arterial phase radionuclide concentration and a normal brain scan has been proven to be a malignant neoplasm.

This series of patients demonstrates that radionuclide cerebral angiogram findings are characteristic but not specific in arteriovenous malformations. The characteristic radionuclide cerebral angiographic pattern we have described in arteriovenous malformations can be seen on occasion in malignant neoplasms that demonstrate a large degree of arteriovenous shunting. In addition, the "hot stroke" syndrome described following cerebral infarction may present this pattern. For these reasons the diagnosis of arteriovenous malformation should not be attempted from the radionuclide cerebral angiographic findings alone. Contrast cerebral arteriograms should be performed to confirm the diagnosis on all patients suspected of having arteriovenous malformations by radionuclide cerebral angiographic findings.

CONCLUSIONS

Radionuclide cerebral angiographic findings observed in arteriovenous malformations may be char-

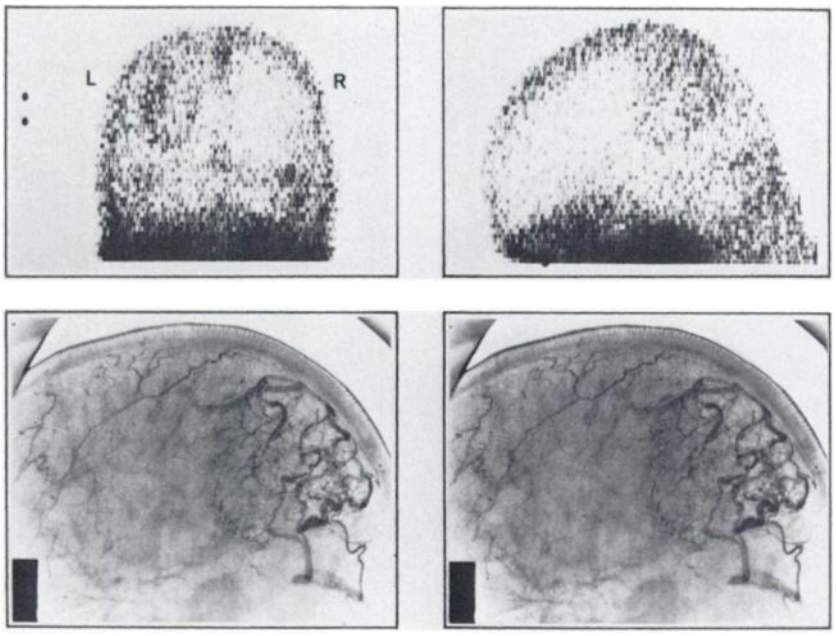

FIG. 8. Brain scan and cerebral arteriogram of glioblastoma multiforme. (Left) Posterior; (right) left lateral. Note multiple shunts.

TABLE 2. REPORTED SERIES OF RADIONUCLIDE CEREBRAL ANGIOGRAMS IN ARTERIOVENOUS MALFORMATIONS OF THE BRAIN*

Year reported	Reporting institution	Radionuclide angiograms positive/performed	Authors
1968	Montreal Gen. Hospital	4/4	Rosenthall (5)
1970	Univ. of Minnesota	3/3	Binet and Loken (10)
1971	Bowman Gray	4/5	Meschan, et al (9)
1972	Univ. of Chicago Univ. of Rochester	10/11	Landman and Ross (3)
1972	Bowman Gray	13/13	Cowan (6)†
1974	Duke University	16/16	Tyson, et al
Total		50/52	
Percent positive		96%	

* Nuclide used: ^{99m}Tc.

† This series represents a separate patient population from that reported by Meschan, et al (14).

acterized by increased radionuclide activity at the site of the lesion in the arterial phase followed by decline in radionuclide activity following the venous phase. This pattern may also be observed in malignant gliomas and following cerebral infarction. The radionuclide cerebral angiogram has been demonstrated to be of value in the detection of intracerebral arteriovenous malformations but may not be used as the sole method for establishing a definitive diagnosis.

ACKNOWLEDGMENTS

The authors wish to thank Anne Godwin for her assistance in the preparation of this manuscript. This work was supported in part by Veterans Administration Training Grant TR-143.

REFERENCES

1. PERRET G, NICHIOKA H: Report on the cooperative study of intracranial aneurysms and subarachnoid hemorrhage. Section VI. Arteriovenous malformations. An analysis of 545 cases of cranio-cerebral arteriovenous malformations and fistulae reported to the cooperative study. *J Neurosurg* 25: 467–490, 1966

2. KELLY DL, ALEXANDER E, DAVIS CH, et al: Intracranial arteriovenous malformations: clinical review and evaluation of brain scans. *J Neurosurg* 31: 422–428, 1969

3. LANDMAN S, ROSS P: Radionuclides in the diagnosis of arteriovenous malformations of the brain. *Radiology* 108: 635–639, 1973

4. MAYNARD CD, WITCOFSKI RL, JANEWAY R, et al: "Radioisotope Arteriography" as an adjunct to the brain scan. *Radiology* 92: 908–912, 1969

5. ROSENTHALL L: Radionuclide diagnosis of arteriovenous malformations with rapid sequence brain scans. *Radiology* 91: 1185–1188, 1968

6. COWAN R: Cerebral dynamic studies. In *Continuing Education Lectures, A Review of Nuclear Medicine*, Atlanta, Ga, Southeastern Chapter of the Society of Nuclear Medicine, 1972, pp 1–20

7. LANE SD, PATTON DD, STAAB EV, et al: Simple technique for rapid bolus injection. *J Nucl Med* 13: 118–119, 1972

8. GOREE JA, DUKES HT: The angiographic differential diagnosis between the vascularized malignant glioma and the intracranial arteriovenous malformation. *Am J Roentgenol Radium Ther Nucl Med* 90: 512–521, 1963

9. MESCHAN I, LYTLE WP, MAYNARD CD, et al: Statistical relationship of brain scans, cervicocranial dynamic studies, and cerebral arteriograms. *Radiology* 100: 623–629, 1971

10. BINET EF, LOKEN MK: Scintiangiography of cerebral arteriovenous malformations and aneurysms. *Am J Roentgenol Radium Ther Nucl Med* 109: 707–713, 1970

11. MOODY RA, POPPEN JL: Arteriovenous malformations. *J Neurosurg* 32: 503–511, 1970

12. YARNELL P, BURDICK D, SANDERS B: The "Hot Stroke". *Arch Neurol* 30: 65–69, 1974

13. LASSEN NA: The luxury-perfusion syndrome and its possible relation to acute metabolic acidosis localised within the brain. *Lancet* 2: 1113–1115, 1966

14. MAYNARD CD: Personal communication, April 1974